is very important in order to obtain realistic results. The usual choice is at the solvent separated point along the PMF profile. This can be somewhat subjective, but careful graphical analysis can identify this point. The ion is found to be solvent-separated at a 6.5-Å separation distance. Integrating from the 0-Å separation distance as the reference to 6.5 Å yields a K_a value of 49 700 (or −6.4 kcal/mol). Our calculated free energy of association is slightly higher than the experimental value of −5.5 ± 0.6 kcal/mol, but compares with experiment quite well. The calculated value represents only the value obtained by binding in the z direction. Binding in the $-z$ direction should be similar, but alternate routes could provide differing binding constants. These other routes may involve slight changes in the x or y directions, but given the stabilizing structural features observed along the reaction path (e.g., buttressing of methanols between nonactin and the ion), which would be destabilized owing to motions in these directions, we are reasonably confident that the path we have studied is a low-energy pathway. Furthermore, the excellent agreement between the experimental and theoretical binding constants gives us confidence that our pathway and the structural features along it give a reasonable representation of nonactin/potassium complexation process.

Conclusions

We find that by using an effective two-body potential we are able to accurately represent the association of an ion with the antibiotic ionophore nonactin. Further improvements could be made especially in the treatment of polarization effects[27] which would allow for an improved representation of the solvation of potassium and sodium in methanol. Regardless, we have been able to reasonably reproduce the relative binding affinities of nonactin for potassium and sodium (−1.0 ± 0.8 kcal/mol (calc) versus −2.0 ± 0.7 kcal/mol (expt)[7]), and, furthermore, we have been able to accurately reproduce the absolute free energy of binding of potassium to nonactin (−6.4 kcal/mol (calc) versus −5.5 ± 0.6 kcal/mol (expt)[7]).

We present a schematic of the association process of nonactin with potassium in Figure 13. Initially nonactin displaces two methanol molecules and replaces them with carbonyls (O). This gives the first minimum at 4.0 Å, which has five methanols and two nonactin carbonyls associated with the ion. Passing through the transition state at 2.75 Å gives the most stable point on this profile at a 1-Å separation distance. To reach this point three methanols are displaced and are replaced by two carbonyl oxygens (O) and two ether oxygens (OE). Thus, at this point we have a net coordination of eight.

The remarkable feature of this PMF is the role that the carbonyl oxygens play in the recognition process. Initially the ion is six-coordinated (first solvation shell) in methanol and nonactin recognizes the first coordination shell of the ion by making two hydrogen-bonding contacts at around 6.5-Å separation (nonactin carbonyl to methanol hydrogen). Two of the methanols in this shell are then displaced and replaced by two carbonyls from nonactin, while the other two carbonyls dynamically form and break hydrogen bonds with the two interior methanols. The final displacement brings into play two of the ether oxygens, which overall play a limited role.

Given our results it is interesting to speculate on how nonactin might function in a biomembrane. Nonactin is likely to rest on the membrane surface, and once it recognizes an ion it becomes balled up, which makes it hydrophobic. The ionophore then penetrates into the bilayer and makes its way to the other side. Interestingly, nonactin has two equivalent faces that allows the molecule to traverse the bilayer without rotating to expose the face into which the ion had originally entered. To complete the whole transport function, nonactin must finally ball up again without an ion and makes its way across the membrane to the starting face. This pathway is schematically given in Figure 14. Similar schemes have been proposed for other ionophores.[1]

Acknowledgment. Helpful discussions with Liem Dang and Olaf Andersen are greatly appreciated. This research was supported by the ONR (N00014-90-3-4002) and ACS-PRF (23225-G6,4) and their support is acknowledged. We also thank the Pittsburgh Supercomputer Center for CRAY YMP time and the Center for Academic Computing for IBM 3090 time.

Registry No. K$^+$, 7440-09-7; Na$^+$, 7440-23-5; nonactin, 6833-84-7.

Supplementary Material Available: Listing of important dihedral angles in nonactin which were analyzed statically at each point on the PMF profile (6 pages). Ordering information is given on any current masthead page.

Ab Initio Calculations on *m*-Quinone. The Ground State Is a Triplet

Raymond C. Fort, Jr.,[1a] Stephen J. Getty,[1b] David A. Hrovat,[1b] Paul M. Lahti,[1c] and Weston Thatcher Borden*,[1b]

Contribution from the Departments of Chemistry, University of Washington, Seattle, Washington 98195, and University of Massachusetts, Amherst, Massachusetts 01003.

Received March 27, 1992

Abstract: The geometries of the $^3B_2$, $^1B_2$, and $^1A_1$ states of *m*-quinone (**2**) have been optimized, using the 6-31G* basis set at, respectively, the UHF, ROHF, and GVB levels. Partial geometry reoptimization was carried out at the π-SDCI level. Calculations that included σ,π correlation also were performed. The triplet is predicted to be the ground state by 10.4 kcal/mol at the π-SDCI level and by 7.6 kcal/mol at the σ-S, π-SDCI level of theory. A value of 9.5 kcal/mol is calculated for the singlet-triplet splitting in *m*-quinodimethane (**1**) at the π-SDCI level. The apparent lack of effect on the singlet-triplet splitting of replacing the CH_2 groups in **1** by the oxygens in **2** is discussed.

In agreement with experiment[2] and with qualitative theoretical expectations,[3] previous calculations[4,5] on *m*-quinodimethane[6] (**1**) have found this diradical to have a triplet ground state. Previous calculations also have revealed that the replacement of the CH_2

---

(1) (a) On leave at the University of Washington from the Department of Chemistry, University of Maine, Orono, ME 04469. (b) University of Washington. (c) University of Massachusetts.

(2) Wright, B. B; Platz, M. *J. Am. Chem. Soc.* **1983**, *105*, 628.

(3) Borden, W. T.; Davidson, E. R. *J. Am. Chem. Soc.* **1977**, *99*, 4587. Review: Borden, W. T. In *Diradicals*; Borden, W. T., Ed.; Wiley: New York, 1982; pp 1–72.

0002-7863/92/1514-7549$03.00/0

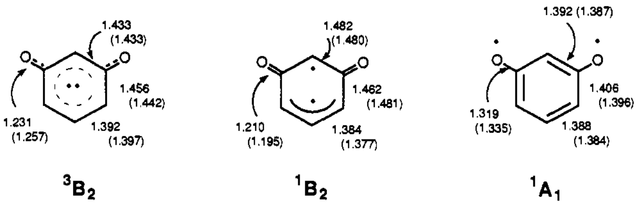

Figure 1. π-SDCI bond lengths for the states of **2** (UHF/ROHF/GVB values in parentheses).

groups in 2,4-dimethylenecyclobutane-1,3-diyl (**3**) by the two oxygens in (**4**) is capable of changing the spin multiplicity of the ground state from triplet to singlet.[7,8] An obvious question then is whether the pair of oxygens in *m*-quinone (**2**) also might result in a single ground state for this diradical.

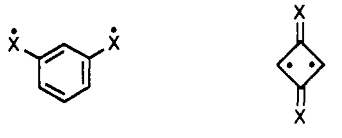

1, X = CH_2
2, X = O

3, X = CH_2
4, X = O

To the best of our knowledge, **2** has not yet been prepared.[6,9] However, semiempirical calculations by Lahti, Rossi, and Berson predict **2** to have a triplet ground state.[5] Indeed, the singlet-triplet splitting was calculated by them to be slightly larger in **2** (18 kcal/mol) than in **1** (15 kcal/mol). In order to verify this prediction and to investigate why substitution of oxygen for methylene apparently has a much smaller effect in **1** than in **3**, we undertook ab initio calculations on **2**.

Computational Methodology

Full geometry optimizations in C_{2v} symmetry were carried out for the three lowest-lying states ($^3B_2$, $^1B_2$, $^1A_1$) of **2** using the 6-31G* basis set.[10] The optimizations on the $^3B_2$ state were performed at both the ROHF and UHF level[11] and those on the $^1B_2$ at the ROHF level; those on $^1A_1$ were GVB-PP(1) calculations. These geometry optimizations were carried out with the Gaussian 90 package of ab initio programs.[12,13]

The geometries of the three states of **2** were then partially reoptimized in C_{2v} symmetry at the π-SDCI level, employing the MELDF suite of ab initio programs.[14] Starting from the ROHF wave functions for the $^3B_2$ and $^1B_2$, and the two-configuration (TC)SCF wave function for the $^1A_1$ species, the orbitals of the virtual space were transformed into K orbitals.[15] Single-point CI calculations, including all single and double π excitations from one reference configuration for $^3B_2$ and $^1B_2$ and from two for $^1A_1$, were performed. These calculations involved 10 461 spin-adapted configurations for $^3B_2$, 6621 for $^1B_2$, and 6192 for $^1A_1$. The π-SDCI energies were fitted to quadratic potential energy functions to determine the optimal C_{2v} geometries. Owing to the size of **2**, the CH bond lengths were frozen at the UHF, ROHF, or GVB optimized values as appropriate. The cross-ring distances between C1 and C3 and between C4 and C6 and bond angles external to the ring at these four carbons also were frozen.

Table I. Energies of Singlet and Triplet States of **2**

state	geometry	calculation	E, hartree	E'_{rel}, kcal/mol
$^3B_2$	ROHF	ROHF	−379.1855[a,b]	0
	π-CI	π-SDCI	−379.3058[c]	0
	π-CI	π-SDQCI	−379.3232[d]	0
	π-CI	σ-S, π-SDCI	−379.5306	0
	π-CI	(σ-S, π-SD)QCI	−379.5742[d]	0
$^1B_2$	ROHF	ROHF	−379.1758	6.1
	π-CI	π-SDCI	−379.2892[e]	10.4
	π-CI	π-SDQCI	−379.3024[d]	13.0
	π-CI	σ-S, π-SDCI	−379.5184	7.6
	π-CI	(σ-S, π-SD)QCI	−379.5599[d]	9.0
$^1A_1$	GVB	GVB	−379.1745	6.9
	π-CI	π-SDCI	−379.2725[f]	20.9
	π-CI	π-SDQCI	−379.2830[f]	25.2
	π-CI	σ-S, π-SDCI	−379.4911	24.8
	π-CI	(σ-S, π-SD)QCI	−379.5310[d]	27.1

[a] UHF energy at the UHF-optimized geometry = −379.2412 hartrees. [b] At the optimized UHF geometry the ROHF energy is 6.3 kcal/mol higher. [c] At the UHF geometry the π-SDCI energy is 1.1 kcal/mol higher. [d] Using the Davidson formula[16] to estimate the effect of quadruple excitations. [e] At the ROHF-optimized geometry the π-SDCI energy is 0.31 kcal/mol higher. [f] At the GVB-optimized geometry the π-SDCI energy is 0.44 kcal/mol higher.

To investigate the effect of σ,π correlation on the relative energies of the low-lying electronic states of **2**, we performed additional CI calculations on each state at its π-SDCI optimized geometry. In addition to single and double π excitations, single σ excitations into the virtual K orbitals were permitted, but with no more than two excitations allowed in any given configuration. For these σ-S, π-SDCI calculations, the virtual orbital space was truncated by removing the number of K orbitals of each symmetry equal to the number of d orbitals of the same symmetry. In all, 125 533 configurations were incorporated into the CI wave function for the $^3B_2$ state, 73 295 for the $^1B_2$, and 62 680 for the $^1A_1$.

Results and Discussion

The optimized geometries for the low-lying states of **2** are given in Figure 1. The energies are given in Table I. Figure 1 shows that reoptimization at the π-SDCI level has little effect on the geometries of these states.

The optimized C–C bond lengths shown in Figure 1 suggest the schematic depictions of the π-bonding that are indicated in the figure. As expected,[3,4] $^3B_2$ has the most highly delocalized wave function, whereas $^1B_2$ has highly localized C–O π bonds. In contrast, in $^1A_1$ there appears to be little C–O π-bonding.

In singlet states of diradicals, unlike the case in triplets, the nonbonding electrons are not prevented by the Pauli exclusion principle from appearing in the same region of space. Therefore, minimization of the Coulombic repulsion between the nonbonding electrons in a singlet state usually results in their localization to different regions of space.[3,4] The electronic structures of $^1B_2$ and $^1A_1$ represent two different ways of achieving this localization.

As shown in Table I, at the ROHF/GVB level the two singlet states have nearly the same energy, and the $^3B_2$ state at the ROHF optimized geometry is about 6–7 kcal/mol lower. These levels of theory provide no correlation between the nonbonding electrons and the bonding electrons of opposite spin, and so are not reliable for predicting relative energies of the three states. This kind of electron correlation in the π space is introduced in the π-SDCI calculations.

At the π-SDCI level, $^3B_2$ is predicted to be the ground state of **2**, lying 10.4 kcal/mol below the $^1B_2$ state, which is calculated to be below $^1A_1$ by about the same amount of energy. Since the nonbonding electrons in $^3B_2$ are the most delocalized, this state is afforded the greatest amount of stabilization by inclusion of π-SDCI. The nonbonding electrons in $^1A_1$ are the most localized;

---

(4) Kato, S.; Morokuma, K.; Feller, D.; Davidson, E. R.; Borden, W. T. *J. Am. Chem. Soc.* **1983**, *105*, 1791.

(5) Lahti, P. M.; Rossi, A. R.; Berson, J. A. *J. Am. Chem. Soc.* **1985**, *107*, 2273.

(6) Reviews: Platz, M. In *Diradicals*; Borden, W. T., Ed.; Wiley: New York, 1988, pp 195–258. Berson, J. A. In *The Chemistry of Functional Groups—Quinones*; Patai, S., Ed.; Wiley: New York, 1988; Vol. 2, p 455.

(7) Du, P.; Hrovat, D. A.; Borden, W. T. *J. Am. Chem. Soc.* **1989**, *111*, 3773.

(8) Calculations also predict a significant reduction in the singlet-triplet splitting in trimethylenemethane on replacing a CH_2 group with oxygen to form oxyallyl: Coolidge, M. B.; Yamashita, K.; Morokuma, K.; Borden, W. T. *J. Am. Chem. Soc.* **1990**, *112*, 1751.

(9) Both *m*-quinomethane and a naphthoquinomethane have been generated and each is found to have a triplet ground state: Rule, M.; Matlin, A. R.; Seeger, D. E.; Hilinski, E. F.; Dougherty, D. A.; Berson, J. *Tetrahedron* **1982**, *38*, 787.

(10) Hariharan, P. C.; Pople, J. A. *Theor. Chim. Acta* **1973**, *28*, 212.

(11) UHF calculations are preferred to ROHF for optimizing the geometries of triplet states: Borden, W. T.; Davidson, E. R.; Feller, D. *Tetrahedron* **1982**, *38*, 737.

(12) Frisch, M. J.; Head-Gordon, M.; Trucks, G. W.; Foresman, J. B.; Schlegel, H. B.; Raghavachari, K.; Robb, M.; Binkley, J. S.; Gonzalez, C.; Defrees, D. J.; Fox, D. J.; Whiteside, R. A.; Seeger, R.; Melius, C. F.; Baker, J.; Martin, R. L.; Kahn, L. R.; Stewart, J. J. P.; Topiol, S.; Pople, J. A. Gaussian, Inc.: Pittsburgh, PA, 1990.

(13) Complete listings of the optimized geometries are available as supplementary material.

(14) Developed at the University of Washington by L. McMurchie, S. Elbert, S. Langhoff, and E. R. Davidson, and modified by D. Feller and D. Rawlings.

(15) Feller, D.; Davidson, E. R. *J. Chem. Phys.* **1981**, *74*, 3977.

hence it is stabilized the least by CI. With the inclusion of the Davidson correction for the estimated effect of quadruple excitations,[16] at the π-SDCI optimized geometry of each state the triplet is predicted to lie below the $^1B_2$ state by 13 kcal/mol, and $^1B_2$ is computed to be lower in energy than $^1A_1$ by about 12 kcal/mol.

Inclusion of σ–π correlation usually provides the most stabilization for the state with the most ionic π wave function.[7] The polarity of C–O π bonds makes the $^1B_2$ state the most polar state, since it has the most C–O π-bonding. For the same reason the least polar state is the $^1A_1$, since it has the least C–O π-bonding. Consequently, inclusion of σ–π correlation at the σ-S, π-SDCI level affords the most stabilization for $^1B_2$ and the least for $^1A_1$.

However, despite the selective stabilization of $^1B_2$ relative to $^3B_2$ by inclusion of σ–π correlation, at the σ-S, π-SDCI level the triplet still is predicted to be the ground state of **2** by 7.6 kcal/mol and by 9.0 kcal/mol when the estimated effect of quadruple excitations is included via the Davidson correction. Thus, unlike the case in **4**, where substitution of oxygen for each methylene group of **3** is predicted unequivocally to cause the singlet to become the ground state,[7] **2**, like **1**,[4] is calculated to have a triplet ground state.

The difference between the effect of heteroatom substitution in **1** and in **3** can be understood easily. The greater strength of C–O π bonds, as compared to C–C, is the major factor that stabilizes the lowest singlet relative to the triplet when both methylene groups of **3** are replaced by oxygen to form **4**.[7] When one methylene group of trimethylenemethane is replaced by oxygen to form oxyallyl, the lowest singlet is stabilized similarly.[8] The triplet state of a nondisjoint diradical generally has more delocalized π bonds than do the low-lying singlet states;[3] hence, a singlet can profit more from the replacement of methylene by oxygen than can the triplet, *but only if the singlet state has a strong π bond to the methylene group where the replacement is made.*

The bonding in the lowest singlet state of **1** ($^1A_1$)[4] and of **3** (^1A_g)[7] is adequately depicted in the resonance structure shown for each of those species. Thus, in the lowest singlet state of **1** little π-bonding exists between the exocyclic methylene groups and the ring, whereas in the lowest singlet of **3** each exocyclic methylene is strongly π-bonded.[17]

Consequently one would not expect substitution of the oxygens of **2** for the methylene groups of **1** to stabilize the $^1A_1$ state relative to the $^3B_2$ state. In fact, since the $^3B_2$ state has partial π bonds to the exocyclic methylenes, it should be stabilized relative to this singlet by the substitution. The singlet state that should be selectively stabilized by oxygen substitution, relative to the triplet, is the $^1B_2$, which has strong π bonds to the methylene groups in **1**.

In order to test this explanation of the difference between the effect of heteroatom substitution in **1** and **3**, we needed to compare the relative energies of the three lowest-lying states of **1** with those of the same three states of **2**. Our previous calculations on **1**[4] were done without polarization functions, and we did not compute the energy of the $^1B_2$ state. Therefore, we performed π-SDCI/6-31G* calculations on **1**.

Since we had found π-SDCI geometry optimization to have a minimal effect on the geometries of the states of **2**, our calculations on **1** employed the UHF optimized geometry for $^3B_2$, the ROHF for $^1B_2$, and the GVB for $^1A_1$. The optimized C–C bond lengths are shown in Figure 2,[13] and the energies are given in Table II.

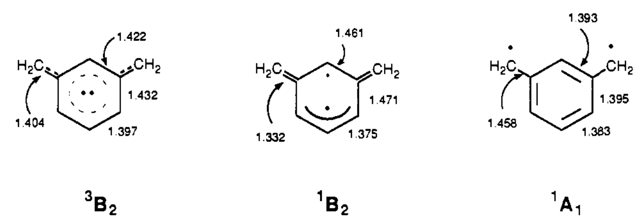

Figure 2. UHF/ROHF/GVB bond lengths for the states of **1**.

Table II. Energies of Singlet and Triplet States of **1**

state	calculation	E, hartrees	E_{rel}, kcal/mol
$^3B_2$	ROHF[a,b]	−307.5220	0
	π-SDCI	−307.6289	0
	π-SDQCI	−307.6455[c]	0
$^1B_1$	ROHF	−307.4856	22.8
	π-SDCI	−307.5913	23.6
	π-SDQCI	−307.6047[c]	25.6
$^1A_1$	GVB	−307.5227	−0.4
	π-SDCI	−307.6138	9.5
	π-SDQCI	−307.6226[c]	14.4

[a] At the UHF-optimized geometry. [b] UHF energy at UHF geometry = −307.5755 hartrees. [c] Using the Davidson formula[16] to estimate the effect of quadruple excitations.

Comparison of the results in Tables I and II confirms our analysis of the effect of oxygen substitution in the conversion of **1** to **2**. At the π-SDCI level the $^1A_1$ state of **1** is calculated to lie 9.5 kcal/mol above the $^3B_2$, in excellent agreement with our previous results.[4] The energy of $^1B_2$ is computed to be 14.1 kcal/mol higher still. At the π-SDQCI level these energy differences change to 14.4 and 11.2 kcal/mol, respectively.

At the π-SDCI level of theory, on going from **1** to **2** the energy difference between $^1A_1$ and $^3B_2$ increases by 11.4 kcal/mol, whereas the difference between $^1B_2$ and $^3B_2$ decreases by 13.2 kcal/mol. The roughly 25-kcal/mol change in the relative energies of the two singlets results in $^1B_2$ lying more than 10 kcal/mol below $^1A_1$ in **2**. The energy difference between these two singlet states in **2** increases to about 12 kcal/mol at the π-SDQCI level, to about 17 kcal/mol when σ,π correlation is added, and to about 18 kcal/mol when the effect of quadruples on the σ-S, π-SDCI energy is estimated.

Thus, although our calculations predict a triplet ground state ($^3B_2$) for both **1** and **2**, they predict a change in the nature of the lowest single state: from $^1A_1$ (which has an aromatic benzene ring and very weak exocyclic π bonds) in **1**, to $^1B_2$ (which has the two nonbonding electrons largely localized in the six-membered ring and strong exocyclic π bonds) in **2**.[18] The finding that the energy difference between the lowest singlet and the triplet is relatively unaffected on going from **1** to **2**, is a consequence of the selective stabilization by oxygen of an excited singlet of **1**, which becomes the lowest singlet state of **2**.

That the lowest singlet state of **2** is $^1B_2$ has an important consequence. Whereas in **4** the lowest singlet (^1A_g) and triplet ($^3B_{2u}$) have different orbital occupancies, which allow the singlet to fall below the triplet in energy,[7] the lowest singlet and triplet of **2** each have one nonbonding electron in a $3b_1$ orbital and the other in a $2a_2$. These two MOs have atoms in common,[19] and their nondisjoint nature leads to the unequivocal prediction[3] of a triplet ground state for **2**. Our prediction of a triplet ground state for **2** thus can be made without concern that it might be

---

(16) Davidson, E. R. In *The World of Quantum Chemistry*; Daudel, R., Pullman, B., Eds.; Dordrecht: The Netherlands, 1974.

(17) The special stability of the aromatic ring in **1** would be sacrificed by formation of strong π bonds to the exocyclic methylene groups. In contrast, localization of the nonbonding electrons to the exocyclic methylene groups in **3** would generate an antiaromatic cyclobutadiene moiety. This difference between the two diradicals is responsible for the difference in π-bonding in the lowest singlet state of each, and it also results in some differences between the bond lengths in the lowest triplet states. At the UHF/6-31G* optimized geometry of each triplet, we find that the $^3B_2$ state of **1** has bonds to the external methylene groups that are about 0.03 Å longer, and adjacent C–C ring bonds that are an average of 0.03 Å shorter, than the corresponding bonds in the $^3B_{2u}$ state of **3**.

(18) The same result was obtained by previous semiempirical calculations,[5] but the lowest singlet state of **2** was erroneously reported to be a closed-shell, $^1A_1$ state, rather than an open-shell, $^1B_2$ state.

(19) Strictly speaking, only the $3b_1$ and $2a_2$ orbitals for $^3B_2$ really have significant coefficients on common atoms. In the $^1B_2$ state, minimization of the Coulombic repulsion between the pair of singlet-coupled, nonbonding electrons in these orbitals causes the orbitals to be largely localized to different sets of atoms.[3] This localization is responsible for more localized π-bonding in the $^1B_2$ than in the $^3B_2$ state.

altered by further improvements in the computational methodology employed to calculate the singlet–triplet energy separation.

Acknowledgment. We thank the National Science Foundation for support of this research and for a grant that made possible the purchase of the Convex C-2 computer on which many of these calculations were performed. We thank also the San Diego Supercomputer Center for a generous grant of time on the Cray Y-MP with which others of the calculations were effected. R.C.F. thanks the Board of Trustees of the University of Maine System for a sabbatical leave during the course of which his portion of the present work was accomplished.

Supplementary Material Available: Tables of UHF/ROHF/GVB/π-CI geometries of structures **1** and **2** (2 pages). Ordering information is given on any current masthead page.

Interaction of the Aryl Tetrasaccharide Domain of Calicheamicin $\gamma_1{}^{I}$ with DNA: Influence on Aglycon and Methidiumpropyl-EDTA·Iron(II)-Mediated DNA Cleavage

J. Aiyar, S. J. Danishefsky, and D. M. Crothers*

Contribution from the Department of Chemistry, Yale University, New Haven, Connecticut 06511.

Received March 24, 1992

Abstract: This study assesses individual interactions of the oligosaccharide and aglycon domains of calicheamicin $\gamma_1{}^{1}$, an antitumor antibiotic, with DNA. Preincubation of DNA with the full carbohydrate domain followed by incubation with aglycon leads to sequence-selective cleavage not observed in the absence of the carbohydrate.

Calicheamicin $\gamma_1{}^{I}$ (**1**) and esperamicin are DNA minor groove binding drugs bearing enediyne ("aglycon" sector) and carbohydrate moieties.[1,2] The drugs produce sequence-selective double-stranded cleavage at homopyrimidine/homopurine tracts on DNA duplexes,[3] via a 1,4-dehydrobenzene diradical produced in the aglycon sector upon bioreductive alkylation and cyclization.[2,4] Earlier studies demonstrated that the carbohydrate moieties of the drugs determine their sequence selectivity,[3b,5-8] possibly via an extended conformation spanning the minor groove.[5a]

In the research described herein we sought to learn whether the carbohydrate domain of the drug calicheamicin $\gamma_1{}^{1}$, independent of the aglycon, binds to a DNA duplex substrate (see Figure 1). The DNA sequence was selected on the basis of its demonstrated capacity to exhibit sequence-selective binding and cleavage by **1**.[7] The carbohydrate selected for this purpose was the methyl glycoside **2**, recently synthesized in two laboratories.[9] DNase I footprinting of **2** has provided evidence that the oligosaccharide does recognize drug-binding (**1**-binding) sites, but with perhaps lower specificity than the drug.[10] The availability through synthesis of the carbohydrate sector mimic **2**, as well as aglycon sector analog **5**,[11] allowed us to probe, more deeply, their individual interactions with the DNA substrate, thereby providing inferences as to their synergism in the intact drug.

We first examined the action of intact drug **1** on the DNA duplex which had been preincubated with oligosaccharide **2**. This experiment produced a dramatic decrease in drug-mediated cleavage (Figure 2, lanes 1–3). No such effect was observed when either sucrose (Figure 2, lanes 4 and 5) or even the azafuranose rearranged product of esperamicin trisaccharide[12] (**4**; Figure 2, lanes 6 and 7) was used. The trisaccharide domain mimic[13,14] (**3**) of esperamicin, a drug with markedly less sequence specificity than calicheamicin,[2c,d,15] inhibited drug-mediated (**1**-mediated) specific cleavage only to a very small extent, and at the highest concentration (1.5 mM) of oligosaccharide used.

Affinity of the oligosaccharide **2** for specific sequences on the DNA was determined by footprinting analyses of the top (hom-

---

[1] For a comprehensive review of the enediyne field, see: Nicolaou, K. C.; Dai, W.-M. *Angew. Chem.* **1991**, *103*, 1453; *Angew. Chem., Int. Ed. Engl.* **1991**, *30*, 1387.

[2] (a) Lee, M. D.; Dunne, T. S.; Siegel, M. M.; Chang, C. C.; Morton, G. O.; Borders, D. B. *J. Am. Chem. Soc.* **1987**, *109*, 3464. (b) Lee, M. D.; Dunne, T. S.; Chang, C. C.; Ellestad, G. A.; Siegel, M. M.; Morton, G. O.; McGahren, W. J.; Borders, D. B. *J. Am. Chem. Soc.* **1987**, *109*, 3466. (c) Golik, J.; Clardy, J.; Dubay, G.; Groenewold, G.; Kawaguchi, H.; Konishi, M.; Krishnan, B.; Ohkuma, H.; Saitoh, K. I.; Doyle, T. W. *J. Am. Chem. Soc.* **1987**, *109*, 3461. (d) Golik, J.; Dubay, G.; Groenewold, G.; Kawaguchi, H.; Konishi, M.; Krishnan, B.; Ohkuma, H.; Saitoh, K. I.; Doyle, T. W. *J. Am. Chem. Soc.* **1987**, *109*, 3462.

[3] (a) Zein, N.; Sinha, A. M.; McGahren, W. J.; Ellestad, G. A. *Science* **1988**, *240*, 1198. (b) Zein, N.; Poncin, M.; Nilakantan, R.; Ellestad, G. A. *Science* **1989**, *244*, 697.

[4] Lockhart, T. P.; Comita, P. B.; Bergman, R. C. *J. Am. Chem. Soc.* **1981**, *103*, 4082.

[5] (a) Walker, S.; Valentine, K. G.; Kahne, D. *J. Am. Chem. Soc.* **1990**, *112*, 6428. (b) Walker, S.; Kahne, D. *J. Am. Chem. Soc.* **1991**, *113*, 4716.

[6] Hawley, R. C.; Kiessling, L. L.; Schreiber, S. L. *Proc. Natl. Acad. Sci. U.S.A.* **1989**, *86*, 1105.

[7] Drak, J.; Iwasawa, N.; Danishefsky, S.; Crothers, D. M. *Proc. Natl. Acad. Sci. U.S.A.* **1991**, *88*, 7464.

[8] Nicolaou, K. C.; Schreiner, E. P.; Stahl, W. *Angew. Chem.* **1991**, *103*, 566; *Angew. Chem., Int. Ed. Engl.* **1991**, *30*, 585.

[9] (a) Nicolaou, K. C.; Groneberg, R. D.; Miyazaki, T.; Stylianides, N. A.; Schulze, T. J.; Stahl, W. *J. Am. Chem. Soc.* **1990**, *112*, 8193. (b) Halcomb, R. L.; Boyer, S. H.; Danishefsky, S. J. *Angew. Chem.*, in press.

[10] Nicolaou, K. C.; Tsay, S.-C.; Suzuki, T.; Joyce, G. F. *J. Am. Chem. Soc.*, following paper in this issue.

[11] Haseltine, J. N.; Cabal, M. P.; Mantlo, N. B.; Iwasawa, N.; Yamashita, D. S.; Coleman, R. S.; Danishefsky, S. J.; Schulte, G. K. *J. Am. Chem. Soc.* **1991**, *113*, 3850.

[12] Golik, J.; Wong, H.; Krishnan, B.; Vyas, D. M.; Doyle, T. W. *Tetrahedron Lett.* **1991**, *32*, 1851.

[13] Halcomb, R. L.; Wittman, M. D.; Olson, S. H.; Danishefsky, S. J.; Golik, J.; Wong, H.; Vyas, D. *J. Am. Chem. Soc.* **1991**, *113*, 5080.

[14] (a) Golik, J.; Wong, H.; Vyas, D. M.; Doyle, T. W. *Tetrahedron Lett.* **1989**, *30*, 2497. (b) Van Laak, K.; Rainer, H.; Scharf, H. D. *Tetrahedron Lett.* **1990**, *31*, 4113.

[15] (a) Long, B. H.; Golik, J.; Forenza, S.; Ward, B.; Rehfuss, R.; Dabrowiak, J. C.; Catino, J. J.; Musial, S. T.; Brookshire, K.; Doyle, T. W. *Proc. Natl. Acad. Sci. U.S.A.* **1989**, *86*, 2. (b) Sugiura, Y.; Uesawa, Y.; Takahashi, Y.; Kuwahara, J.; Golik, J.; Doyle, T. *Proc. Natl. Acad. Sci. U.S.A.* **1989**, *86*, 7672.

0002-7863/92/1514-7552$03.00/0